ELSEVIER

Journal of Alloys and Compounds 323–324 (2001) 297–302

Journal of ALLOYS AND COMPOUNDS

www.elsevier.com/locate/jallcom

New ecological pigments in the Ca–Yb–S system

M.D. Hernández-Alonso[a], A. Gómez-Herrero[b], A.R. Landa-Cánovas[b], A. Durán[c], F. Fernández-Martínez[c], L.C. Otero-Díaz[a,b,*]

[a]*Departamento Química Inorgánica, Fac. CC. Químicas, Universidad Complutense de Madrid, Madrid, E-28040, Spain*
[b]*CME Luis Bru, Universidad Complutense de Madrid, Madrid, E-28040, Spain*
[c]*Escuela Universidad Técnica Industrial, Universidad Politécnica, Ronda de Valencia 3, Madrid, E-28017, Spain*

Abstract

The microstructure (via SEM, TEM and X-ray powder data), magnetic and optical colour parameters of the solid solution $Ca_{1-x}Yb_{2/3x}\square_{1/3x}S$ (with $0\leq x\leq 1$) were investigated. Several samples have been prepared by heating mixtures of CaS and Yb_2S_3 (white and yellow colour, respectively) in sealed silica tubes and by sulphurating the amorphous precursors of both metals in a H_2S+Ar steam in CS_2. Scanning electron micrographs show small particle size, up to 5 μm, in the second preparation samples. All the samples are bluish-green coloured and suitable for pigment applications. For $x\approx 0.11$, the cation vacancies (produced during the process $3Ca^{2+}\rightarrow 2Yb^{3+}+?$) are randomly distributed and a decrease in the **NaCl-type** unit cell volume of 1% was observed accompanied by cluster formation in the image. For $x=0.33$, we observed a cubic superstructure of NaCl-type, with $a=2a_0=11.280(3)$ Å; $a_0=5.50$ Å for pure CaS. Higher x values give mixtures of two phases: (a) rhombohedral symmetry, $a_r=7.987(6)$ Å and $\alpha=58.6$ (°), and (b), orthorhombic **Yb_3S_4-type**, with $a=12.641(8)$ Å, $b=3.844(4)$ Å and $c=13.01(1)$ Å.

Keywords: Chemical synthesis; Scanning and transmission electron microscopy; X-Ray diffraction; Optical properties; Magnetic measurements

1. Introduction

In the last few years, the research devoted to the structural study (solid solutions, long-range order and short-range order) of transition and rare-earth sulphides [1–8] has had implications in the development of inorganic pigments based on sulphides of light rare earth elements which has importance due to their less toxic chemical behaviour and variable colour emission [9]. Recently, Rhône-Poulenc [10] has patented it as a safer red pigment for plastics; it is used now as a substitute for cadmium sulfoselenide and it presents good optical, thermal and chemical characteristics. The study of alkali-doped cerium sulphide and the pure compound was carried out by Mauricot et al. [11]. Perrin et al. [12] claim that the red colour of γ-Ce_2S_3 is associated with localised Ce 4f→5d excitations. This year Roméro et al. [13] have studied the stabilisation of γ-Ce_2S_3 at low temperature.

In 1965, Flahaut et al. [14] carried out an extensive study of the solid solutions made of alkaline sulphides (M=Mg–Ca, Sr–Ba) with NaCl-type structure and doping with Ln_2S_3 (Ln: lanthanide element). For 1:1 ratio, i.e. MLn_2S_4, they found several structural types: Th_3P_4, spinel (both with cubic symmetry), $CaFe_2O_4$ and Yb_3S_4 (the last two orthorhombic). Single crystals of the ternary calcium ytterbium compound, $CaYb_2S_4$ were synthesized by Carpenter et al. [15] and the structure given corresponds to the Yb_3S_4-type [16]. More recently, El Fadli et al. [17] studied three crystals by single crystal X-ray diffraction: $Ca_{3.86}Yb_{0.09}S_4$, $Ca_{3.10}Yb_{0.60}S_4$ and $Ca_{2.30}Yb_{1.14}S_4$; the first two correspond to NaCl-type structure with $a=$ 5.691(2) Å and 5.67(3) Å, respectively, while the third corresponds to a two times NaCl superstructure, with $a\approx 2a_0=11.246(2)$ Å. These samples were prepared at 1473 K from the binary CaS and Yb_2S_3 sulphides.

In this work, we shall present our results concerning the preparation, structure–microstructure, optical colour parameters and magnetic measurements of several phases in the ternary Ca–Yb–S system; these phases can be formulated as $Ca_{1-x}Yb_{2/3x}\square_{1/3x}S$ with $0\leq x\leq 1$ and they are NaCl-type solid solution derivatives. Our purpose is to characterise the samples by using more sensitive techniques such as electron microscopy and associated techniques (XEDS, CBED, microdiffraction) in order to search

*Corresponding author.

0925-8388/01/$ – see front matter
PII: S0925-8388(01)01118-5

for SRO and LRO in the form of modulated structures as happens in other similar systems, such as Yb^{2+}–Yb^{3+}–S [5,6].

2. Experimental methods

2.1. Sample preparation

Two types of samples belonging to the solid solution $Ca_{1-x}Yb_{2/3x}\square_{1/3x}S$ with NaCl related structure and variable nominal composition as $0 \leq x \leq 1$ have been prepared.

The first type of sample (A) was prepared using the binary sulphides as starting products. Firstly, CaS (NaCl-type, $a_0 = 5.695$ Å, $V = 184.7$ Å^3 and grey colour) was prepared by induction heating of a carbon crucible containing $CaCO_3$ (4N.ROC-RIC) in a stream of 5% H_2S+95% Ar at 1473 K for 2 h. Yb_2S_3 (α-Al_2O_3-type, $a = 6.7463(7)$ Å, $c = 18.190(2)$ Å; $V = 717.0(1)$ Å^3; yellow colour) was also prepared in the same furnace from Yb_2O_3 (4 N, Hudson Lab.) in a stream of 5% H_2S+95% Ar at 1773 K for 3 h, followed by annealing in the gas at 1373 K for 5 h, and then cooled to room temperature by switching off the furnace. Mixtures of both binary sulphides, with nominal composition values of $x = 0.10$ (A-1), 0.33 (A-2) and 0.45 (A-3), were pressed into a pellet (6 Tm/cm^2), heated in evacuated sealed silica tubes at 1373 K for 70 h and cooled in air until room temperature. The three samples are bluish-green coloured.

The second type of sample (B) was prepared by sulphurating amorphous precursors in a stream of H_2S/Ar (50 cm^3/min flow) and Ar/CS_2 (20 cm^3/min flow) placed in graphitic boats and heated at 1173 K for 4 h. These were prepared by mixing $CaCO_3$ (A.R., Mercks) and Yb_2O_3 (4 N) dissolved in HNO_3 followed by co-precipitation of both cations with $(NH_4)_2CO_3$. For $x = 0.10$ (B-1) and $x = 0.30$ (B-3) the samples present a green-bluish colour; for higher Yb concentrations, i.e. $x = 0.75$ (B-4) and $x = 0.86$ (B-5), the samples are dark-brown coloured. In one sample, for $x = 0.14$ (B-2), we have used CaC_2O_4 instead of $CaCO_3$ and it is sky-blue colour.

2.2. Experimental techniques

The samples were examined by X-ray powder diffraction (XRPD) using a Siemens K810 diffractometer (Cu Kα radiation) and a D-501 goniometer with a secondary graphite monochromator. Si (5N) was used as an internal standard.

Scanning microscopy studies were carried out using a JEM 6400 SEM operating at 20 kV and fitted with a LINK AN10000 analyser system. Samples for TEM observation were obtained from suspensions ultrasonically dispersed under butanol; one drop of the solution was placed on Cu grids coated with holey carbon films. The resultant TEM specimens were subsequently examined in JEM 2000FX and Philips CM200 FEG electron microscopes, both fitted with XEDS analyser systems.

Optical colour spectra and colour coordinates were obtained with a Luci-100 spectrometer (viewing geometry $d/8°$, 10°-standard observer and D65 Iluminant).

The magnetic susceptibility measurements between 2 and 300 K were carried out on samples with a Quantum Design MPMS-XL SQUID magnetometer applying a magnetic field of 1000 Oe.

3. Results and discussion

3.1. Structure and microstructure studies

In order to obtain the size and morphology of the two types of powder microcrystallites, scanning electron micrographs (SEMs) were taken. In Fig. 1a, sample A-1, $Ca_{0.90}Yb_{0.07}\square_{0.03}S$, has well-shaped crystals. However, for the sample B-1, with the same nominal composition as A-1 but synthesised at a lower temperature by sulphurating the precursors, we observe much smaller crystals forming nearly spherical aggregates; see micrograph of Fig. 1b

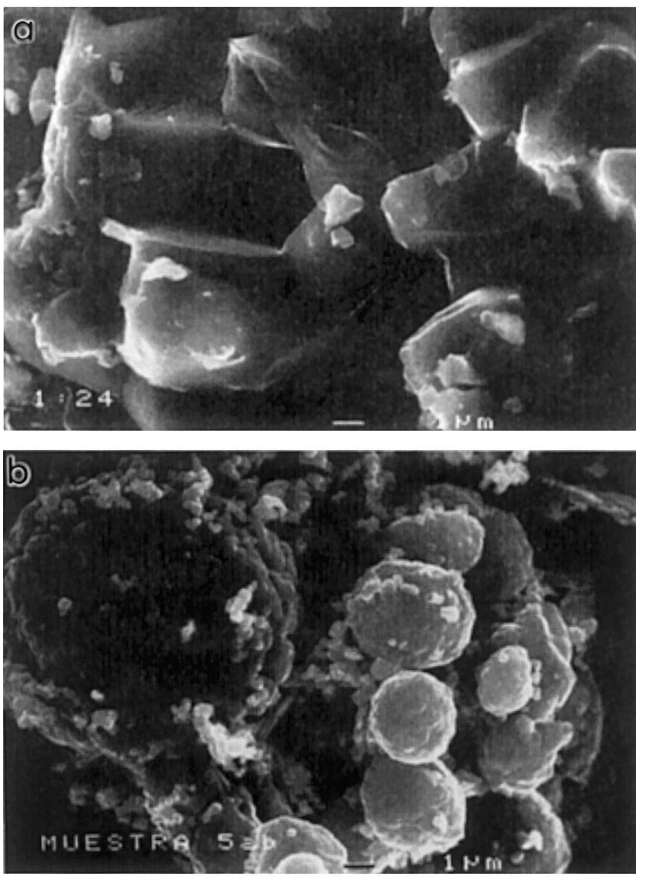

Fig. 1. Scanning electron micrographs of the samples $Ca_{1-x}Yb_{2/3x}\square_{1/3x}S$, with $x = 0.10$, prepared at (a) 1473 K (A-1) and (b) at 1173 K (B-1).

taken at the same magnification as Fig. 1a. The X-ray powder data only show reflections corresponding to NaCl-type basic structure, i.e. CaS with random cation positions occupied by Yb^{3+} according to the process $3Ca^{2+} \rightarrow 2Yb^{3+} + \square$. A decrease of less than 1% in the volume of both unit cells was measured, which can be simply justified from the cationic radius values, Ca^{2+}(VI)=1.14 Å and Yb^{3+}(VI)=1.02 Å [18] with a_0= 5.678(6) Å and a_0=5.689(1) Å for the solid state and precursor reactions, respectively (compare them with a_0= 5.695 Å for pure CaS).

By XEDS analysis, the crystals always give Ca, Yb and S peaks, although the amount of Yb varies from crystal to crystal, even inside the same crystal. Nonetheless, the agreement of the average measured composition with the nominal composition is good: Ca (K)≈39 at.%; Yb (L)≈4 at.% and S (K)≈57 at.%. A high resolution image from one crystal of sample A-1 is presented in Fig. 2. This micrograph was taken with the incident beam parallel to the [100] zone axis of a cubic cell (NaCl-type). In addition to the regular contrast due to two-dimensional fringes of {020} planes with d spacing≈2.9 Å, an intense mottled contrast is observed. It is caused by the possible SRO (short range order) created by clusters due to partial ordering of cation vacancies and/or ordering between both Yb^{3+} and Ca^{2+} ions. Moiré contrast fringes are possibly due to segregation of YbS_x or metallic Yb from the CaS matrix [5,15]. The inset given in the upper right corner of the micrograph corresponds to its fast Fourier transform (FFT) showing the basic cubic reflections (see the indexing given), plus the diffuse satellites due to SRO and multiple diffraction.

The sample B-2, $Ca_{0.86}Yb_{0.09}\square_{0.05}S$, gives a sky-blue colour powder and its SEM image is presented in Fig. 3a,

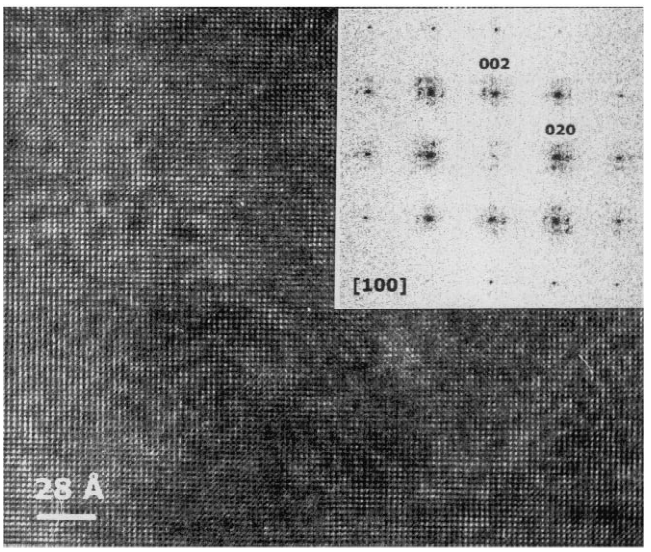

Fig. 2. High resolution transmission electron micrograph of a crystal from sample A-1, $Ca_{1-x}Yb_{2/3x}\square_{1/3x}S$. Notice the mottled contrast typical of clusters. Inset corresponds to its optical diffractogram.

which demonstrates that larger crystals than those in Fig. 1b are formed. The X-ray powder is more complex and multiplets around the basic cubic Bragg reflections are observed; this suggests important changes in the symmetry.

Three types of crystals have been observed. Fig. 3b shows the SAED (Selected Area Electron Diffraction) pattern of one crystal B-2 sample. It can be indexed as the [110] zone axis of a cubic cell with $a=2a_0$=11.3 Å (a_0≈5.6 Å for the CaS). Notice the weak modulation maxima (marked by arrows) that double the periodicity along the ⟨111⟩* direction. Notice as well how these modulation maxima are slightly diffuse and bent due to partial short range order (SRO) although some crystals show sharp satellite reflections, as can be seen in Fig. 3c. The average (three-point analysis) atomic ratio for this crystal is Ca (K)≈46.0%, Yb (L)≈3.4% and S (K)≈ 51.6%. In Fig. 3d we present a CBED (Convergent Beam Electron Diffraction) pattern from a different crystal of the same sample oriented along [001] of a cubic cell. Only the ZOLZ could be observed along this direction, so no three-dimensional symmetry information could be obtained, only projection symmetry information. The FOLZ reflections are very sensitive to disorder or thermal vibrations, so when the crystal has not a very high degree of order they cannot be easily observed. The observed *4mm* projection symmetry is compatible with the *Fm3m* space group.

The samples A-2 and B-3 give the same phases, but with different crystal size and shape morphology, as can be seen in the SEM micrographs shown in Fig. 4a and b, respectively. Fig. 4c shows a microdiffraction pattern of a crystal from sample B-3 along the [001] zone axis of a cubic unit cell symmetry and $a \approx 2a_0$ (a_0≈5.7 Å for pure CaS). Notice the weak superlattice reflections that double the cell. It is important to remark how the Kikuchi lines show a WP (whole pattern) symmetry *m* and not *4mm* due to symmetry degradation from cubic to rhombohedral. By tilting the crystal by ~35°, we get the microdiffraction pattern presented in Fig. 4d, which corresponds to the [111] zone axis. The WP symmetry observed is *3m*; although the symmetry observed in the ZOLZ is *6m* it shows only the projected symmetry, while the symmetry information provided by the FOLZ, which includes three-dimensional symmetry information, reduces the observed symmetry to *3m*. The observed *3m* symmetry is compatible with a cubic crystal along the ⟨111⟩ direction and with a rhombohedral crystal along the [111] direction ([0001] direction in the hexagonal setting). These results confirm the rhombohedral symmetry of the crystal since the *m* WP symmetry observed along [001] does not fit with the *Fm3m* space group of CaS.

After the TEM observations, the X-ray powder data have been refined and we get the following values. For sample A-2, the cubic cell *a* parameter is 11.280(3) Å and the rhombohedral phase values are a_r=7.987(6) Å (≈$2a_0/\sqrt{2}$), α_r=58.6 (°) and V=349(1) $Å^3$.

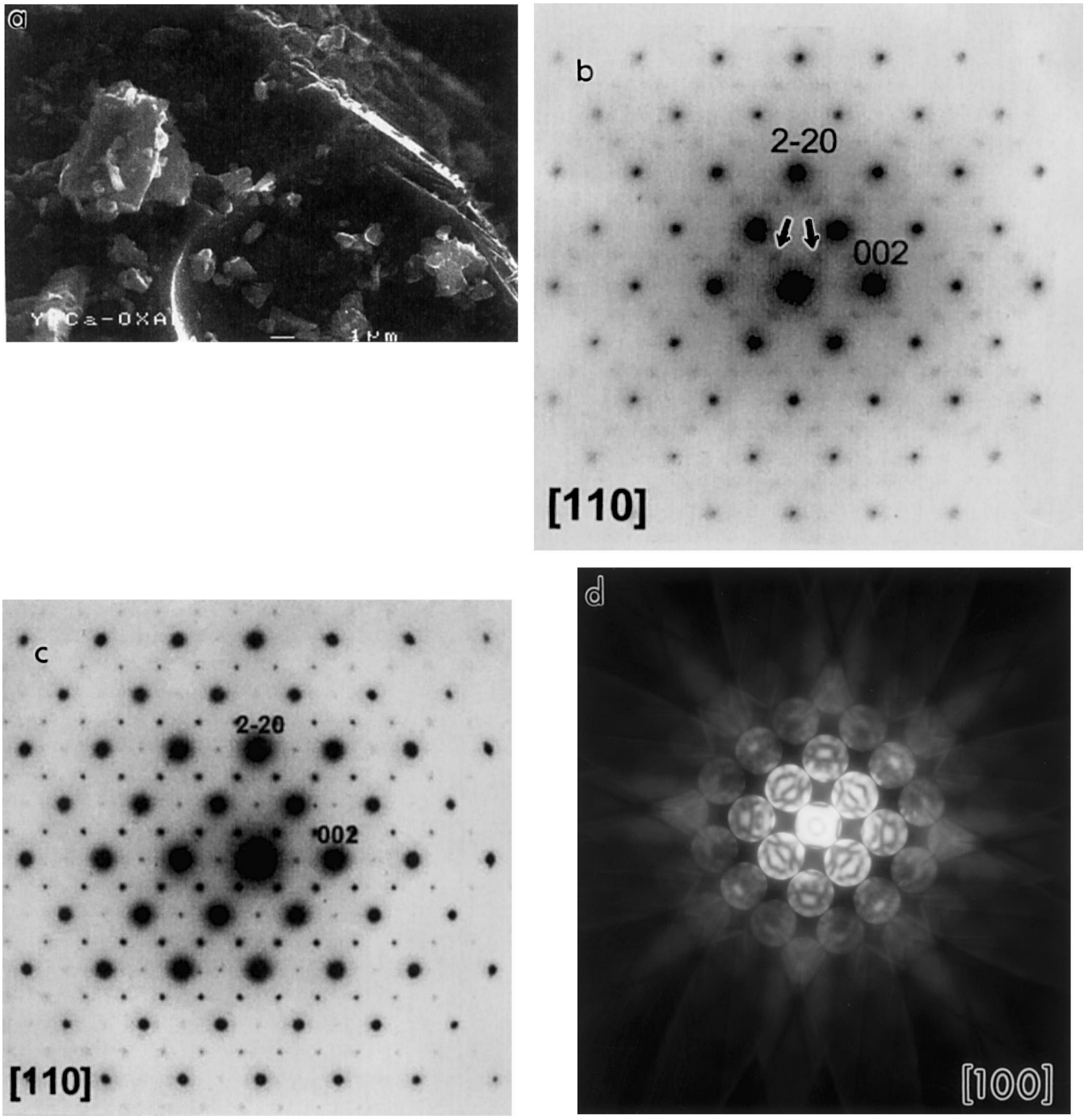

Fig. 3. (a) SEM of the as prepared sample $Ca_{0.86}Yb_{0.09}\square_{0.05}S$ sample. (b) SAED pattern of one crystal from the same sample shown in (a). Notice the diffuse satellite reflections. (c) SAED pattern from a crystal from the same sample shown in (a). Notice the sharp satellite reflections. (d) CBED from a crystal from the same sample show in (a). Notice the *4mm* symmetry.

Sample A-3 also has a blue colour and its structural study reveals a mixture of two phases: a rhombohedral symmetry phase similar to that described previously and also observed by El Fadli et al. [17] and a second phase with orthorhombic symmetry and isostructural to the Yb_3S_4-type; the refined unit cell parameters for this orthorhombic phase are as follows: $a=12.641(8)$ Å, $b=3.844(4)$ Å, $c=13.01(1)$ Å and $V=632.4(7)$ Å^3 which are in good agreement with previous published results [15]. The sample B-4, $CaYb_2S_4$, which formally should be NaCl-type with 25% cation vacancies, presents a dark-brown colour. By X-ray powder diffraction and SAED it was observed to have a Yb_3S_4-type structure [5,15]. The addition of Yb^{2+} to Yb_2S_3, according to a solid solution $Ca_{1-x}Yb_{2/3x}\square_{1/3x}S$ for which Yb_2S_3 (α-Al_2O_3) would be a formally end-member ($x=1.00$), makes the compound metallic and consequently changes the colour from yellow to black.

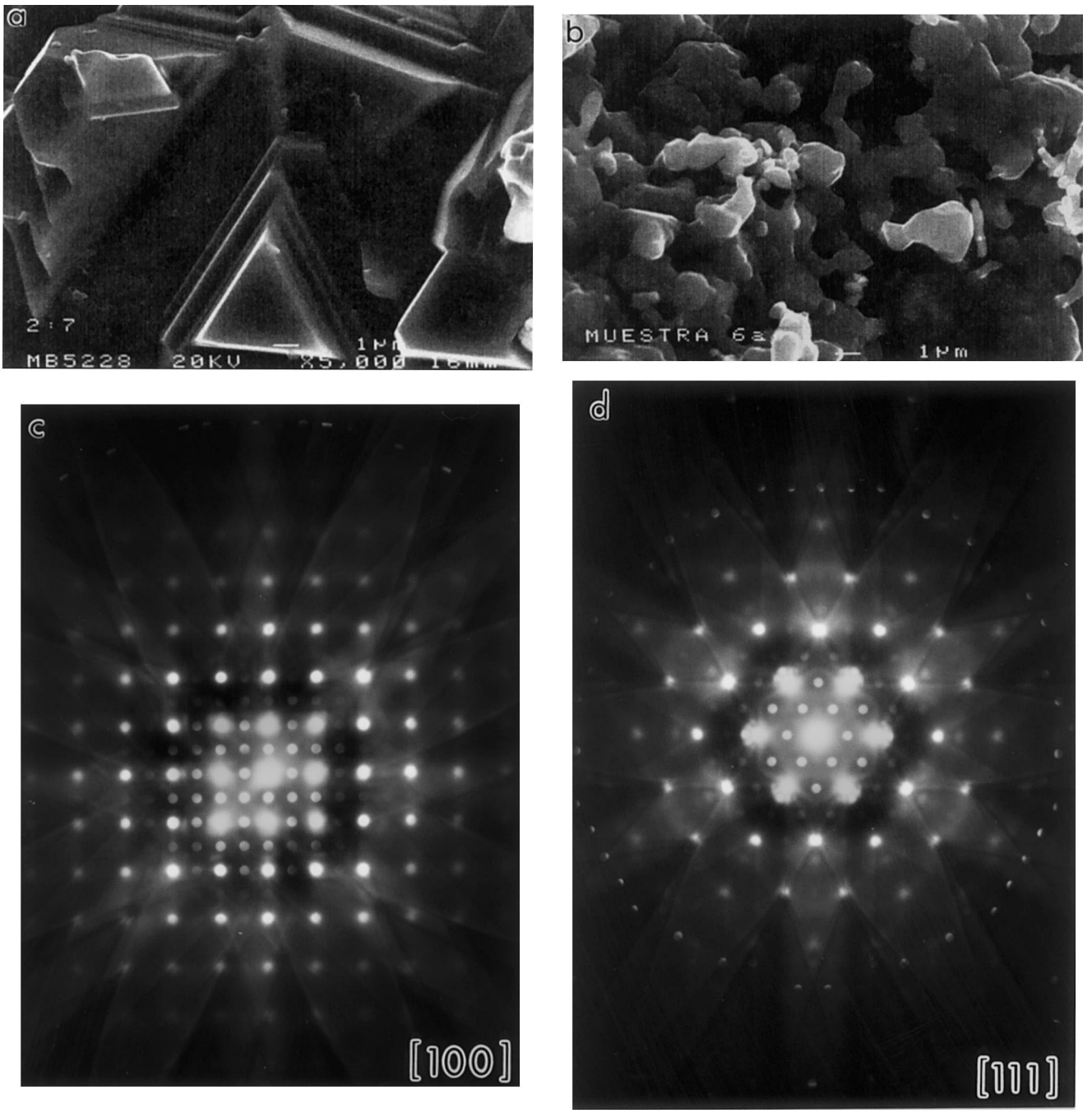

Fig. 4. (a) SEM of the as prepared $Ca_{0.67}Yb_{0.22}\square_{0.11}S$ (A-2) sample. (b) SEM of the as prepared $Ca_{0.70}Yb_{0.20}\square_{0.10}S$ (B-3) sample. (c) Microdiffraction pattern of a crystal from the sample shown in (b). The incident beam is parallel to [100] of a cubic cell. (d) Microdiffraction pattern of the same crystal shown in (c). The ZOLZ and FOLZ are clearly visible.

3.2. Magnetic studies

The temperature dependence of the reciprocal magnetic susceptibility for the different $Ca_{1-x}Yb_{2/3x}\square_{1/3x}S$ compounds is plotted in Fig. 5.

In the linear range between 50 and 300 K, the molar magnetic susceptibilities versus temperature fit the Curie–Weiss law. Plots of χ^{-1} versus T for $Ca_{27}Yb_2S_{30}$ ($x=0.10$) and $Ca_7Yb_2S_{10}$ ($x=0.30$) compounds are shown in Fig. 5 (inset). For $x=0.10$, the Curie temperature, $\theta=53.19$ K and $\mu_{eff}=6.01\mu_B$; for $x=0.30$, $\theta=55.22$ K and $\mu_{eff}=6.54\mu_B$. These values agree with the expected values for the Yb^{3+} free ion. At low temperature the reciprocal magnetic susceptibility deviates downward from linearity and this behaviour can be attributed to crystal field effects.

3.3. Colour studies

The $Ca_{1-x}Yb_{2/3x}\square_{1/3x}S$ phases present a great variety of colours. At low Yb^{3+} contents ($x<0.3$), the colour goes

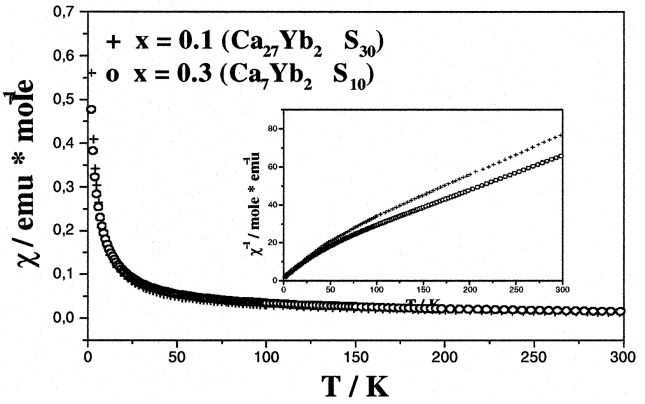

Fig. 5. Magnetic molar susceptibility, χ, and inverse, χ^{-1} (see inset) versus T for the phases $Ca_{1-x}Yb_{2/3x}\square_{1/3x}S$ ($x=0.1$ and $x=0.3$).

from green for $x=0.1$ to blue ($x=0.3$) when the Yb^{3+} content increases. At higher Yb^{3+} content, $CaYb_2S_4$, the colour is reddish. The low values of a^* and b^* coordinates

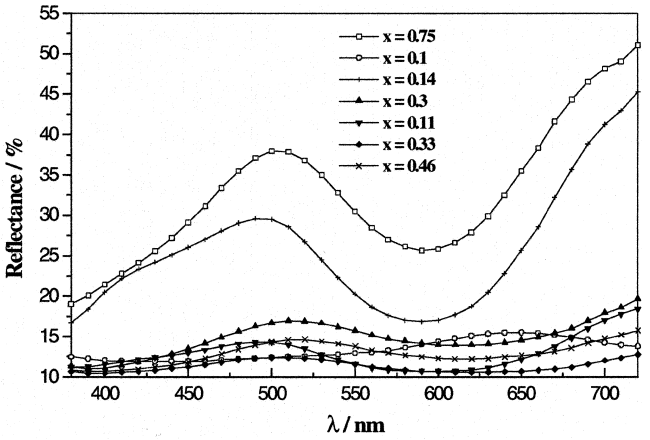

Fig. 6. Reflectance curves for $Ca_{1-x}Yb_{2/3x}\square_{1/3x}S$ samples.

Table 1
Colour parameters for $Ca_{1-x}Yb_{2/3x}\square_{1/3x}S$ compounds

x	% vacancies	L^*	a^*	b^*
0.1	3.3	62.65	−9.37	2.12
0.11	3.7	41.30	−3.72	−2.78
0.14	4.8	54.03	−7.00	−7.26
0.3	10	46.10	−5.84	3.96
0.33	11.1	40.36	−3.44	0.26
0.46	15.4	43.35	−5.06	3.42
0.75	25	43.08	2.78	3.23

are indicative of low colour purity and the medium values of L^* coordinate, which varies from 43 to 63 units, are indicative of a medium colour lightness. The reflectance curves of the samples are given in Fig. 6 and the colour coordinates $L^*a^*b^*$ (CIE–$L^*a^*b^*$-system) and vacancies content are in Table 1.

Acknowledgements

We wish to acknowledge the financial support from CICYT research project MAT-97-0.697.CC01/02.

References

[1] C.N.R. Rao, K.P.R. Pisharody, Prog. Solid State Chem. 10 (1976) 207–270.
[2] H.F. Franzen, Physical Chemistry of Inorganic Crystalline Solids, Springer, Heidelberg, 1986.
[3] J. Burdett, J.F. Mitchell, Prog. Solid State Chem. 23 (1995) 131–170.
[4] J. Flahaut, in: K.A. Gschneidner, L. Eyring (Eds.), Handbook on the Physics and Chemistry of Rare Earths, Vol. 4, 1979, pp. 1–88.
[5] L.C. Otero-Díaz, A.R. Landa-Cánovas, B.G. Hyde, J. Solid State Chem. 89 (1990) 237–259.
[6] L.C. Otero-Díaz, in: R. Saez, P. Caro (Eds.), Rare Earths, Univ. Complutense, Madrid, 1998, pp. 67–92.
[7] R.L. Withers, L.C. Otero-Díaz, J.G. Thompson, J. Solid State Chem. 111 (1994) 283–293.
[8] W.H. Zachariasen, Acta Crystallogr. 2 (1949) 57–59.
[9] P. Maestro, in: R. Saez, P. Caro (Eds.), Rare Earths, Univ. Complutense, Madrid, 1998, pp. 317–332.
[10] J.M. Tourre, Rare Earth Information Center News 'Safer Red Pigments for Plastics', Rhône-Poulenc Chimic, Sept. No. 3 (1993) 1.
[11] R. Mauricot, P. Gressier, M. Evain, R. Brec, J. Alloys Comp. 223 (1995) 130–138.
[12] M.A. Perrin, E. Wimmer, Phys. Rev. B 54 (1996) 2428–2435.
[13] S. Roméro, A. Mosset, P. Macaudière, J.C. Trombe, J. Alloys Comp. 302 (2000) 118–127.
[14] M. Patrie, J. Flahaut, L. Domange, Rev. Hautes Temp. Réfract. 2 (1965) 187–198.
[15] J.D. Carpenter, S.J. Hwu, J. Solid State Chem. 97 (1992) 332–339.
[16] B.G. Hyde, S. Andersson, Inorganic Crystal Structures, Wiley, New York, 1989.
[17] Z. El Fadli, P. Lemoine, A. Tomas, F. Bozon-Verduraz, M. Guittard, Mater. Res. Bull. 30 (1995) 671–678.
[18] R.D. Shannon, Structure and Bonding in Crystals, Vol. II (1981) 53–69.